

## FLEXURAL PERFORMANCE OF REINFORCED CONCRETE BEAMS RETROFITTED USING FERROCEMENT WIRE MESH

Md. Basir Zisan\*, Biplob Kanti Biswas, Md. Abul Hasan, Mithu Chanda, Anindya Dhar

Chittagong University of Engineering & Technology, Raozan, Chittagong, Bangladesh

\*Corresponding author's e-mail: basirzisan@cuet.ac.bd

### Abstract

**Introduction:** Ferrocement is a low-cost material that can be utilized as a replacement for expensive fiber-reinforced polymer (FRP), which is generally used for retrofitting structural and non-structural reinforced concrete members. **The objective** of this paper is to investigate the effectiveness of wire mesh in the retrofitting of flexural members such as reinforced concrete beams. It also investigated the flexural capacity of the beams, which are reinforced with wire mesh as a partial or complete replacement of regular rebar. The orientations and various forms of the wire mesh within the beam section are taken into consideration. The **finite element method** is used to model and analyze the beams. The structural performance of the studied beams, including the load-deflection relationship, first cracked and ultimate cracked loads, crack patterns, and flexural stress, were evaluated using the finite element method. The finite element model of the beam which is reinforced with wire mesh has been verified with experimental results. **The results** show that beams retrofitted with ferrocement or beams in which rebar is replaced by wire mesh have superior flexural performance and low crack depth. The beams retrofitted with wire mesh have a high ultimate load-carrying capacity and ductility. The confinement of three-sided wire mesh improves the flexural performance of the beam. It is observed that flexural performance remains the same when the length of the wire mesh exceeds half of the span length.

**Keywords:** Reinforced concrete beam; wire mesh, retrofitting; load-deflection; stress; crack.

### Introduction

A reinforced concrete structure often exhibits partial damage due to improper design, overloading, corrosion of the reinforcement, and adverse environmental conditions that reduce the serviceability of the structure. It is uneconomical to completely replace or demolish a structure that has impairments. Therefore, retrofitting or restrengthening is necessary to increase the performance at the serviceability levels of a partially damaged structure or structural components. Retrofitting using carbon fiber (CFRP) (Hasan et al., 2020; 2022) or glass fiber (GFRP) polymers (Tanaka et al., 1994), steel plate bonding (Zisan et al., 2011; Oehlers et al., 2000), and concrete jacketing (Kaish et al., 2012; 2013; 2014; Jamil et al., 2013) are generally used to regain the serviceability of deficient concrete structures. The fiber-reinforced polymer known as FRP is widely recommended due to its high strength, effectiveness, and durability (Pham and Al-Mahaidi, 2014; Adhikary and Mutsuyoshi, 2006; Obaidat et al., 2011; Kibria et al., 2020). In addition, the seismic protection efficiency of the FRP retrofitting method is superior to that of traditional retrofitting methods (Al Rjoub et al., 2019; Cao and Nguyen, 2019).

However, application of FRP material in developing countries is rare due to the cost and paucity of FRP materials. On the other hand, ferrocement composites are low-cost and relatively light and have been used in repairing concrete structures (Gaidhankar et al., 2017; Leeansaksiri et al., 2018). Instead of steel or

timber formwork, ferrocement formwork can be used as a permanent component of structural elements (Mataalkah et al., 2017; Shaaban, 2002). It is claimed that ferrocement composite has high strength, homogeneous crack propagation and distribution, including a low crack depth, and high toughness, which makes ferrocement a superior building material (Fahmy et al., 2004; 2012; Husein et al., 2013; Shaheen and Eltehawy, 2017). The ferrocement has sufficient bending capacities, and its well-distributed cracks provide adequate warning before failure (El-Wafa and Fukuzawa, 2008; 2010; Kadir et al. 1997; Al-Sulaimani et al., 1991). Therefore, ferrocement composite could be an important retrofitting tool for reinforced concrete beams.

In previous research, it has been concluded that ferrocement increases the shear capacity while limiting the crack opening (Fahmy et al., 2014). It was reported that RC slabs and masonry walls retrofitted with ferrocement have superior performance under different loading conditions (Hago et al., 2005; Ashraf et al., 2012). The ferrocement composite has been widely used in column jacketing because of high confinement and ductile performance of the column under cyclic and axial loads (Kaish et al., 2012; Abdullah and Takiguchi, 2003). Some researchers claimed that ferrocement enhances the shear bond performance of RC beams (Li et al., 2018; 2013; El-Sayed and Erfan, 2018). The structural behavior of concrete beams fabricated with lightweight core material

and then furnished with various wire mesh has been examined by Shaaban et al. (2011; 2013). It is claimed that these beams are lightweight and cost-effective for the retrofitting of residential buildings. The effectiveness of ferrocement for retrofitting beam-column joints was studied by Shaaban and Seoud (2018) and Li et al. (2013). It indicated that ferrocement layers revealed high ultimate capacities, high ultimate displacements, and large ductility. It did not suffer heavy damage, as was observed for the traditionally reinforced concrete RC beam. Muhit et al. (2021) and Niloy and Islam (2017) conducted flexural tests on RC beams retrofitted with ferrocement and discovered that elastic stiffness and ultimate load carrying capacity increase in ferrocement beams while crack width decreases. The performance of a ferrocement beam due to the orientation of wire in the wire mesh and the amount of layer to be used, was studied by Fahmy et al. (2014), using a U-shaped form of the ferrocement. Shaheen and Eltehawy assessed the effectiveness of U-shaped ferrocement forms (Shaheen et al. 2017). However, these studies do not cover the flexural performance of beams with partial or complete replacement of shear and main reinforcements with ferrocement, which is considered in this study. It also studied the flexural performance of a reinforced concrete beam with a rectangular shape of ferrocement as well as ferrocement placed only at the bottom of the beam.

The use of ferrocement throughout the length of beams is costly. Therefore, the optimum length of the wire mesh is necessary to minimize the cost and labor. In the current study, RC beams retrofitted with a U-shape, closed-rectangular shape ferrocement, or ferrocement added at the bottom of the RC beam were investigated in order to identify the effectiveness of wire mesh in enhancing the flexural performance. In addition, the effectiveness of ferrocement in retrofitting of a beam with partial and complete replacement of conventional steel bars is being investigated. The finite element (FE) method is an efficient tool for analyzing nonlinear behavior such as stress-strain and crack patterns in beams. This method was used by several researchers to analyze the nonlinear flexural characteristics of RC and prestressed concrete beams (Faherty, 1972; Anthony and Wolanski, 2004; Sowmya and Venkatasubramani, 2017). Tjitradi et al. (2017) examined the collapse mechanics and observed the flexural crack generation method. In this study, analysis of beams was carried out using the ANSYS program. The critical load, deflection, and stress at the midspan of the beam, and the crack within the concrete are taken as key parameters to measure the performance of the beam with different ferrocement approaches.

### Finite Element Modelling

Table 1 defines and describes the various types of beams that are modeled and examined in this study. A standard reinforced concrete beam, which is called an experimental beam, is abbreviated as CB. The length of the CB is 1000 mm, and the cross section is 225 × 150 mm. The effective span is assumed to be 900 mm. There are two 12 mm bars at the bottom and two 10 mm bars at the top of the beam. The clear cover for the main steel is assumed to be 25 mm. The diameter of the web reinforcement is 8 mm and it is placed at a rate of 8 mm center-to-center distance. A detailed description of the geometric properties, vertical load, and boundary conditions of the experimental beam is given in (Fig. 1) (Niloy and Islam, 2017; Chanda et al., 2022). The original bar in the experimental beam is substituted by an equal amount of wire mesh by mass in the type I beams (CB-1 and CB-2). In CB-1, only the web reinforcement is replaced, whereas in CB-2, both the web and the main reinforcement are replaced by wire mesh. The wire diameter and the size of the wire mesh opening are given in Table 1. In beam type II, the experimental beam is reinforced with wire mesh, as shown in (Fig. 2), which includes the possible arrangement of wire mesh from a practical point of view. The opening size of the wire mesh is 25 mm, which is used for retrofitting beams in Group II. In group II, the wire mesh is first glued around the periphery of the beam and then tightened using the royal plus and screw (Niloy and Islam, 2017). Then a 25 mm fresh cement mortar cover was used above the wire mesh. Table 2 shows the material. An isotropic and bilinear stress-strain model is assumed for the wire mesh and rebar. To determine the compressive strength of concrete, cylindrical specimens were prepared while experimental control beams were cast. The compressive strength of concrete, 22 MPa, is determined by a laboratory test (Niloy and Islam, 2017). A multilinear isotropic material model specified by Eqns. (1) and (2) as shown in (Fig. 3), is assumed for concrete materials.

$$f = \frac{E_c \varepsilon}{1 + \left( \frac{\varepsilon}{\varepsilon_0} \right)^2} \quad (1)$$

$$\varepsilon_0 = \frac{2f'_c}{E_c} \quad (2)$$

Here,  $f$  is the concrete stress (MPa) at strain  $\varepsilon$ ,  $\varepsilon_0$  is the strain at crushing strength,  $f'_c$  The rupture modulus of concrete is measured by Eq. (3).

$$f_r = 0.7\sqrt{f'_c} \quad (3)$$

The shear transfer coefficient determines the amount of shear transfer through a crack, and it ranges from 0 to 1.0, with 0 representing no shear transfer and 1.0 representing full shear transfer. In this study, the coefficient of open shear transfer

Table 1. Definition of various types of beams

Beam type	Model	Definition of the beam
I	CB	Experimental beam
	CB-1	The web reinforcement of CB is replaced by wire mesh (3.5 mm wire has 25 mm mesh opening)
	CB-2	Both web and main bars of CB are replaced by wire mesh (4.7 mm wire has 25 mm mesh opening)
II	FRB-1	Ferrocement retrofitted beam with square wire mesh along three sides
	FRB-2	Ferrocement retrofitted beam with only bottom side square wire mesh
	FRB-3	Ferrocement retrofitted beam with diagonal wire mesh along three sides
	FRB-4	Ferrocement retrofitted beam with only bottom side diagonal wire mesh
	FRB-5	Ferrocement retrofitted beam with all side square wire mesh

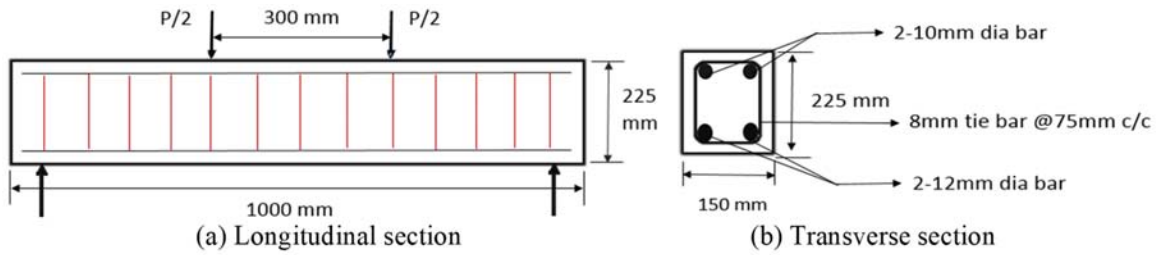


Fig. 1. Geometry and boundary conditions of experimental beam (CB)

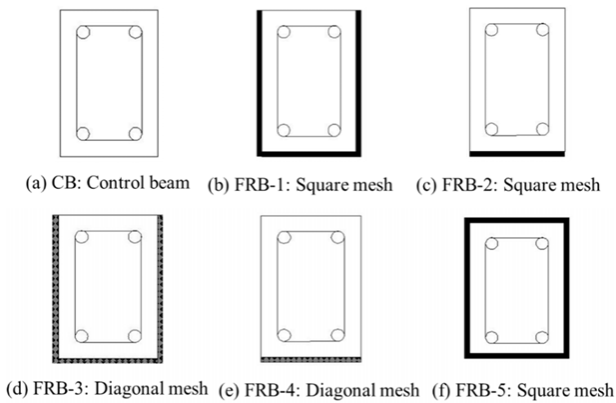


Fig. 2. Cross-section of different retrofitted beams with wire mesh

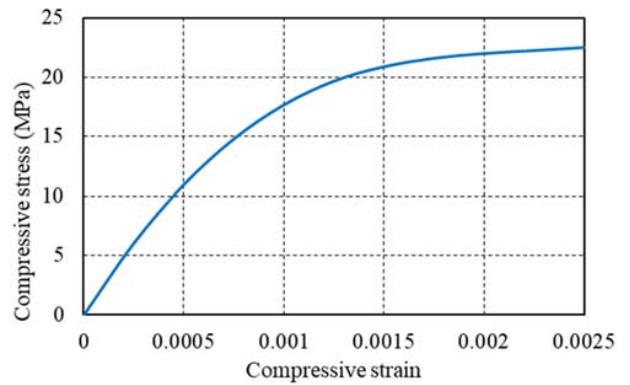


Fig. 3. Multilinear stress-strain curve of concrete

is assumed to be 0.30. It is assumed to be larger than 0.20 to avoid the difficulties related to the convergence of solutions. The close shear transfer coefficient is assumed to be 1.0 (Tjitradi et al., 2017; Si et al., 2008). In the finite element analysis, it is assumed that concrete and steel are isotropic. There is adequate bond strength at the interface of these two materials.

The Solid65 and Link180 elements that are used to discretize the reinforced concrete beam are shown in (Fig. 4) (ANSYS, 2013). Solid65 has eight nodes. It is used to model concrete parts, beam support plates, and loading plates. Link8 has two nodes that are used to model rebar and wire mesh. Each element has three translation degrees of freedom at each node. The FE models of different types of beams are shown in (Fig. 5). The support reactions

Table 2. Material parameters

Material	E [GPa]	$\nu$	$f'_c$ [MPa]	$\sigma_y$ [MPa]	$E_t$ [MPa]	Open Shear Transfer Coefficient	Close Shear Transfer Coefficient
Concrete	20	0.2	22.0	—	—	0.3	1.0
Support and loading plates	200	0.3	—	—	—	—	—
Reinforcement and wire mesh	200	0.3	—	414	20	—	—

$E$ : Elastic modulus,  $\nu$ : Poisson's ratio,  $f'_c$ : Concrete strength,  $\sigma_y$ : Yield strength, and  $E_t$ : Tangent modulus

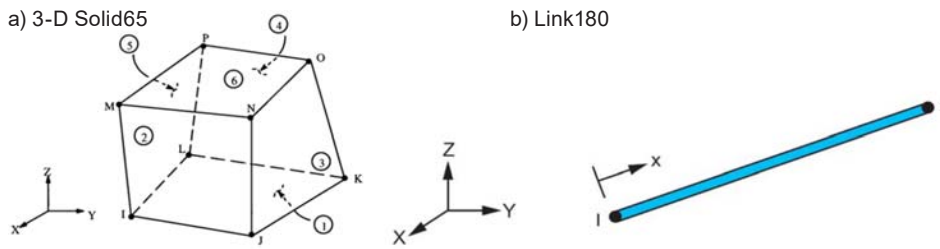


Fig. 4. Element used to discretize reinforced concrete beam

and imposed vertical load at the 1/3<sup>rd</sup> point of the beam are shown in (Fig. 5d). The beam ends are modelled as simple support conditions. Steel and concrete share a common node, and it is assumed that the strain in concrete is equal to the strain in steel. The whole vertical load is divided into two parts and placed at the 1/3<sup>rd</sup> point location of the beam, as shown in (Fig. 5d). The finite element model

has about 3000 elements, around 4000 nodes, and 10,000 degrees of freedom. A convergence analysis is performed to check the competency of the finite element model. It is found that the beam deflection at the midspan is almost the same when the number exceeds 2500 as shown in (Fig. 6). The solution for the analyzed beam is obtained through an incremental nonlinear static analysis.

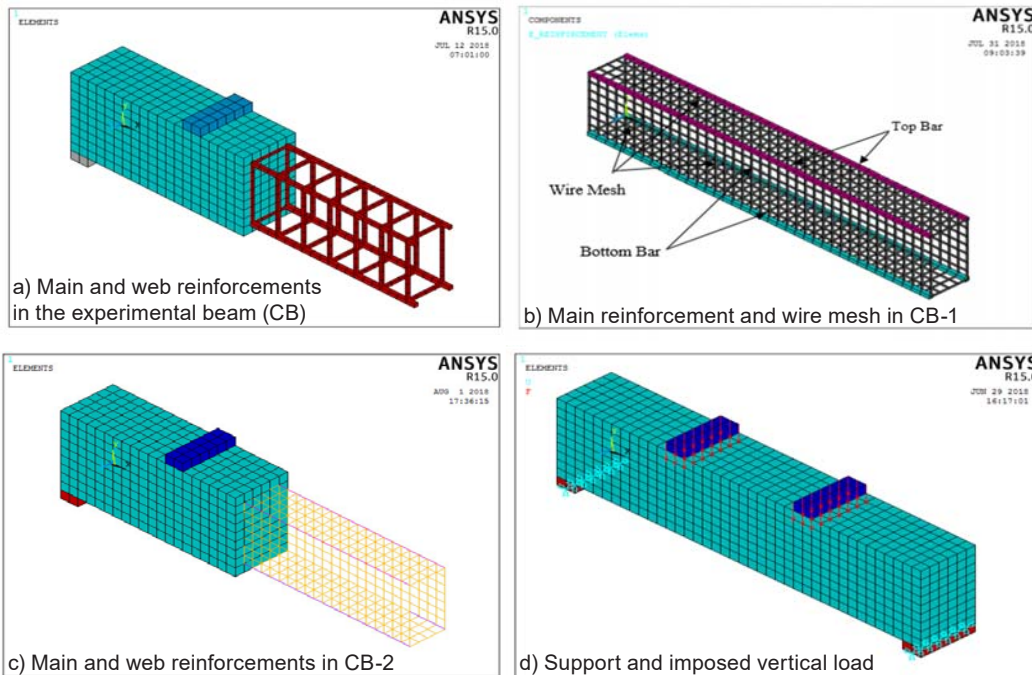


Fig. 5. FE models of beam

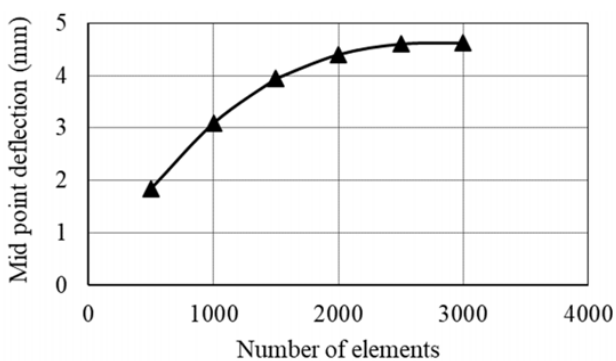


Fig. 6. Convergence test of the FE model

**Model Verification**

The loading test that was conducted using the UTM in the structural engineering laboratory at Chittagong University of Engineering & Technology is shown in (Fig. 7a). The contour for the deformed shape of the experimental beams found from the finite element analysis is shown in (Fig. 7b). A comparison of the displacement at different levels of the load between results of the finite element analysis and that from the loading test is shown in (Fig. 8). A detailed explanation of the model verification can be found in Chanda et al. (2022). From a comparison, it is assumed that the finite

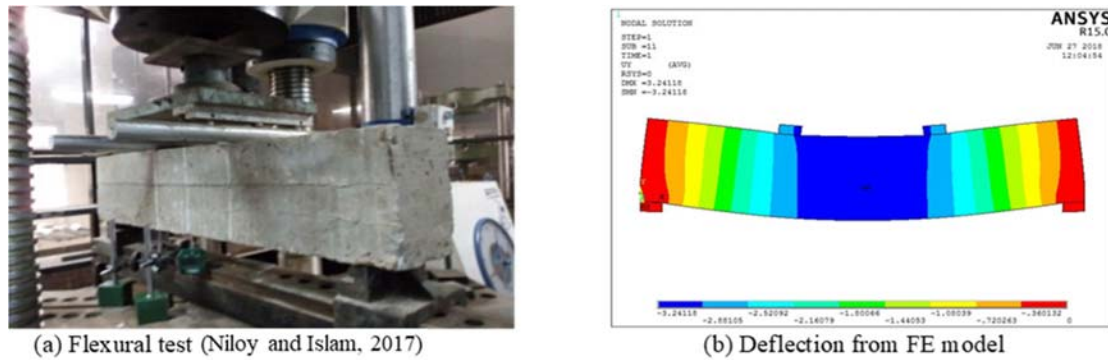


Fig. 7. Deflection of the beam (a) Experiment (b) Finite element analysis

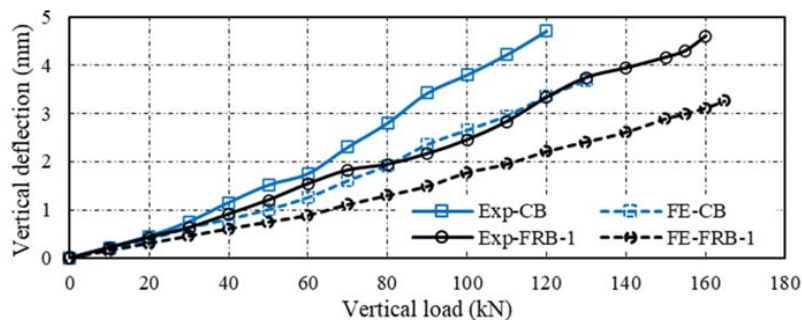


Fig. 8. Comparison of vertical displacement between experimental and finite element analysis at different levels of load

element model is quite accurate and can be used to predict the flexural behavior under vertical load.

#### Performance of the Beams

The load versus vertical displacement for the retrofitted beams and that for the experimental beams until the ultimate cracking point is shown in (Fig. 9a). The deflection is measured at the midspan of the beams. The deflection of beams shows a proportional relationship with the applied load. All beams remain elastic up to a displacement of 1.0 mm, and the elastic capacity lies in the range of 50~70 kN. The capacity of the retrofitted beams is higher than that of the experimental beam (CB), which is more pronounced in the large loading range. The flexural capacities of the FRB-1, FRB-3, and FRB-5 are about 32%~40% greater than those of the CB. Similarly, the capacity of FRB-2 and FRB-4 is about 15% higher than that of the CB. The superior capacity of FRB-1, FRB-3, and FRB-5 beams is expected due to the confinement effect of the U-shaped or rectangular-shaped arrangement of wire mesh. Besides, the flexural capacity of retrofitted beams made with square and diagonal openings of wire mesh does not differ significantly. The figures show that, beyond the displacement of 2.5 mm, the retrofitted beams exhibit large vertical displacement without increasing failure loads where cracks are observed before the failure. It is ensured that ferrocement enhances the ductility of beams, which is necessary for balance control design. It is found that only the replacement of shear

reinforcement by wire mesh has no significance as shown (Fig. 9b). However, when both main and shear reinforcements are replaced by wire mesh, the capacity remains below CB. On the other hand, it increases the ultimate load capacity by 12% and the vertical displacement at the midspan by 25% at ultimate load. Therefore, wire mesh enhances the ductility and flexural capacity of a reinforced concrete beam.

The first and ultimate cracking loads among the retrofitted and experimental beams are shown in (Fig. 10). Imposed loads on the beams at the first and ultimate cracks in the CB and FRB-1, which are found from the experiment, are comparable with the FE computation. The maximum deviation of the FE computation is 12.5% and 7.6% for the first and ultimate cracking loads, respectively. The distribution of flexural cracks under the first and ultimate cracking loads is shown in (Fig. 11). The crack pattern in the beam found in the experiment and that from the finite element analysis are also comparable, which indicates the efficiency of the FE computation. According to (Fig. 10a), the first cracking load found from the loading test is about 80 kN for CB and 90 kN for FRB-1. The ultimate load capacity for the same beams is 120 kN and 160 kN, respectively. It indicates that capacity is increased by 13% and 33% at the first and ultimate cracking stages, respectively, due to the implementation of wire mesh along three sides of the beam. It is

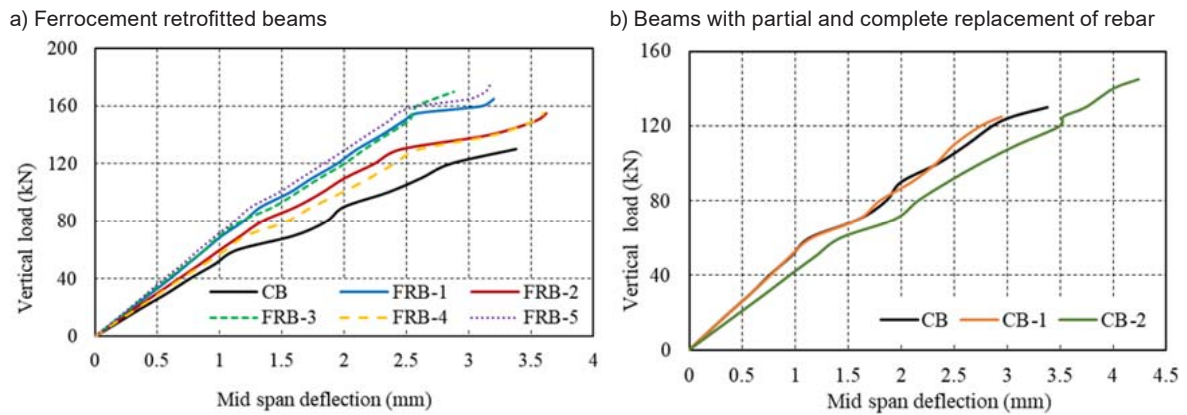


Fig. 9. Load-deflection of the analyzed beams

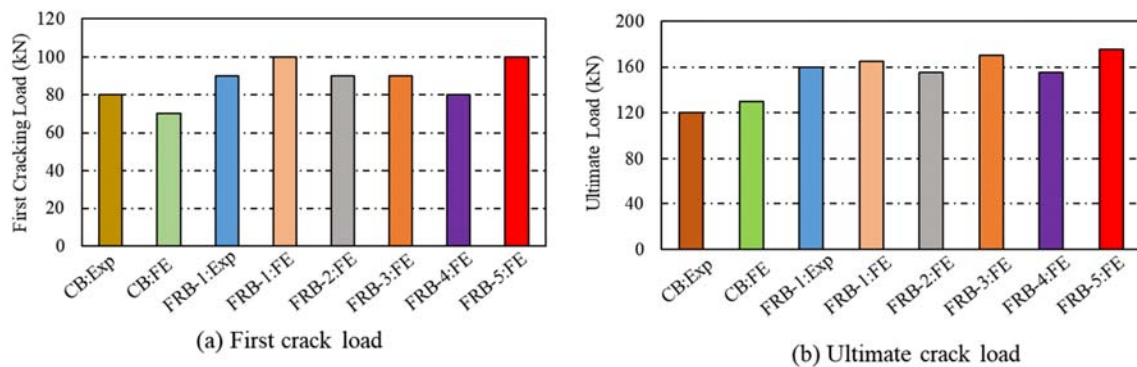


Fig. 10. First and ultimate crack loads in different retrofitted beams

also seen that the first cracking load increases by 42.85%, 28.57%, 28.57%, 14.28%, and 42.85% in the case of FRB-1, FRB-2, FRB-3, FRB-4, and FRB-5, respectively, compared to the numerical result of the CB. The ultimate load capacity of CB and FRB-1 is 130 kN and 165 kN, respectively, and the ultimate capacity increases when wire mesh is placed along three sides (FRB-1, FRB-3, and FRB-5) of the beam. The ultimate capacity of FRB-1, FRB-2, FRB-3, FRB-4, and FRB-5 is 26.93%, 19.23%, 30.76%, 19.23%, and 34.61%, respectively, higher than that of the CB. In general, it can be concluded that wire mesh increases the flexural capacity of a beam by 15%~43% at the first crack condition and

20%~35% at the ultimate load condition, and these capacities increase significantly when wire mesh is used along three sides of the beam.

The first and ultimate flexural crack and its propagation and distribution in different retrofitted beams are shown in (Fig. 12). In comparison with (Fig. 11), the flexural crack is more uniform and well distributed in the beam retrofitted with wire mesh. A similar crack pattern in the CB-1 and CB-2 in comparison with the crack pattern in the CB is observed in (Fig. 13). It indicates that when the main reinforcement is replaced by wire mesh, the length of the crack part of the concrete beam is enlarged. When both shear and flexural reinforcements are

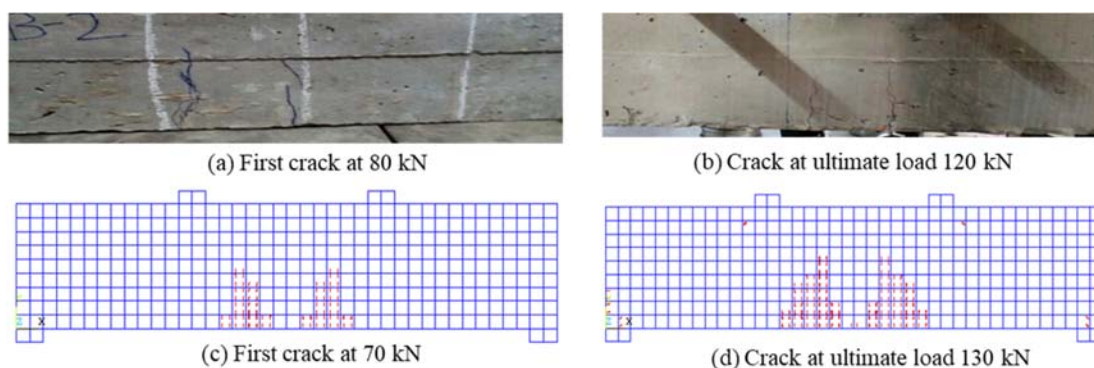


Fig. 11. First and ultimate crack distribution: Experiment beam CB: (a, b) and FE analysis (c, d)

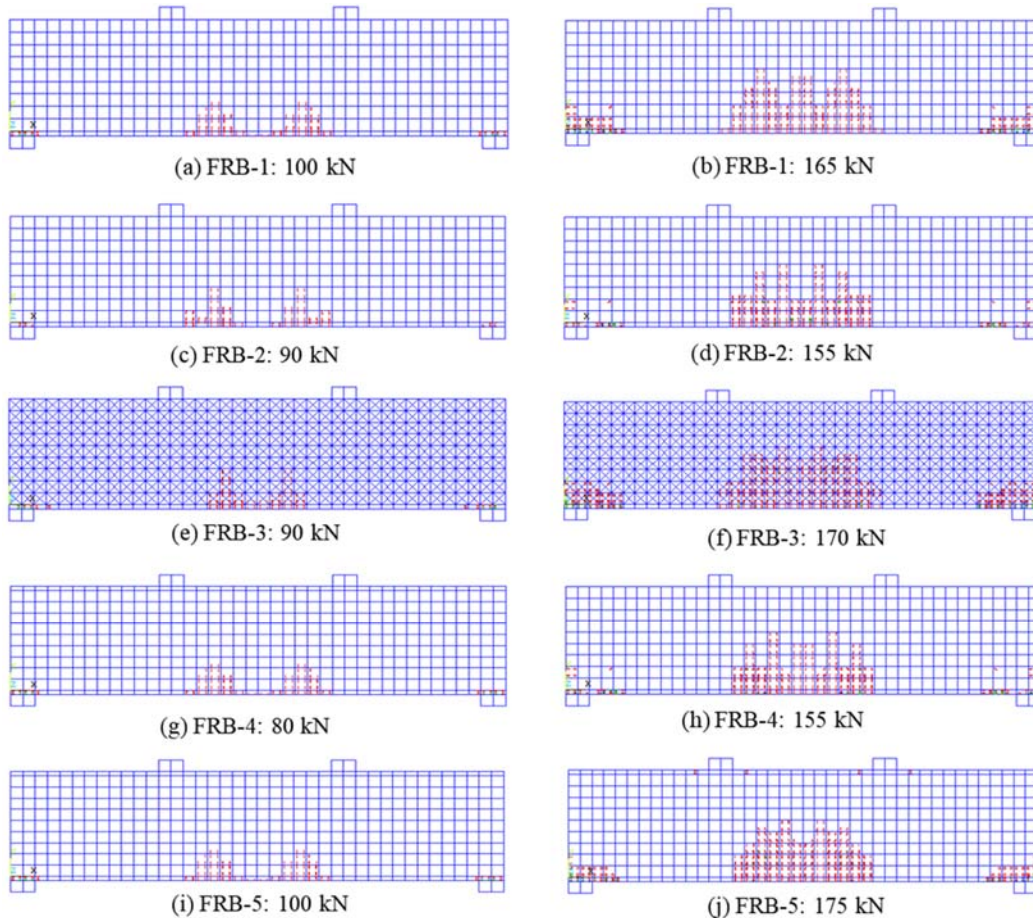


Fig. 12. Flexural crack distribution in different retrofitted beams at first crack and ultimate loads crack

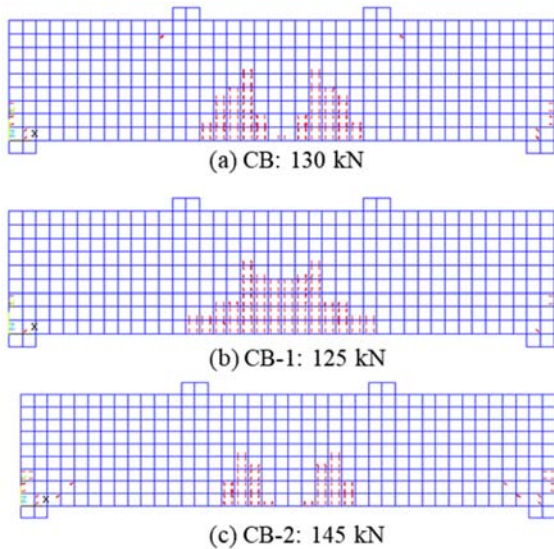


Fig. 13. Flexural crack distribution in different beams

replaced by wire mesh, the crack depth is reduced due to the confinement effect. The crack depth in different beams is shown in (Fig. 14). Under a fixed value of the imposed load, the flexural crack depth is the lowest in the FRB-1, FRB-3, and FRB-5 in

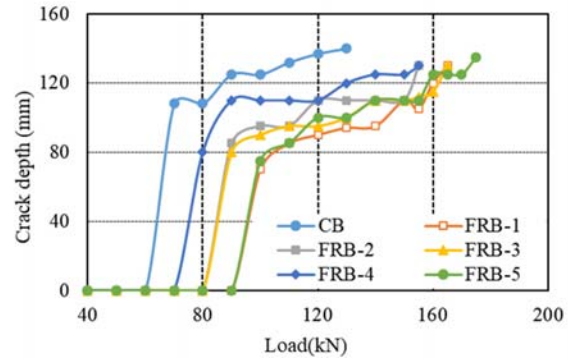


Fig. 14. crack depth in different retrofitted beams

comparison to the CB, FRB-2, and FRB-4. It implies that the flexural tension crack is improved when wire mesh is employed in the reinforced concrete beam.

#### Flexural Stress in Concrete

The flexural stress at the top and bottom surfaces is shown in (Fig. 15a). These stresses are estimated at the middle of the span of the beams. These stresses are proportional to the vertical displacement of the beam. It shows that the top fiber stress (compression) in the CB is comparable with that of the CB-1. The maximum value of compression

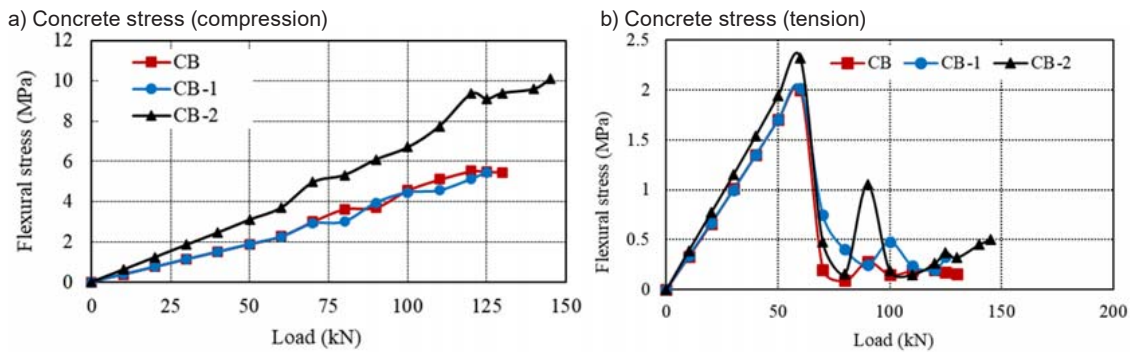


Fig. 15. Flexural stress in different experimental beams

stress in CB-1 is 5.9 MPa at a failure load of 125 kN. The compression stress in the CB-2 at the same level of vertical load is about two times that of the CB or CB-1. The flexural stress (tension) at the mid-span location is shown in (Fig. 11b). It shows that a beam reinforced with wire mesh is capable of sustaining a high bending force. The first crack within the beams is observed at 60 kN, until which the stress within the beam is proportional to the strain. Concrete stress (tension) drops significantly and moves to zero due to an increase in vertical load after the first crack appears. The concrete stress remains close to zero because the tension force is carried by the reinforcement. The flexural stress in retrofitted beams with different layouts of wire mesh in comparison with the stress in the experimental beam is given in (Fig. 16). The peak ultimate compressive and tensile stresses in the retrofitted beams are comparable to those of the CB and lie between 5.0~6.0 MPa and 2.0 MPa, respectively. It means that the stress in the retrofitted beams is not significantly changed when reinforced with wire mesh. After the first flexural crack, the tensile stress in the bottom concrete becomes unpredictable.

**Optimum Length of Wiremesh**

The use of wire mesh along the entire length of a partially damaged beam is uneconomical. Therefore, the optimum length of the wire mesh for satisfactory flexural performance is of concern. In the

current study, the wire mesh length is defined as a percentage of the span of the beam. The optimum length is the length of the wire mesh beyond which the stress and deflection remain unchanged under a fixed flexural load. The optimum length is determined using the incremental load procedure. The maximum load is assumed to be 140 kN. The stress is measured at the tip of the major crack, while the deflection is at the middle of the span length. The midspan deflection in the retrofitted beams with different lengths of the wire mesh is shown in (Fig. 17a). The rate of displacement decreases when the length of the wire mesh is increased. For a length exceeding 50%, the displacement is almost the same. Similarly, flexural stress, as shown in (Fig. 17b) remains the same when length exceeds 40%. In general, the influence of wire mesh length is negligible when the length of wire mesh exceeds 50%. Therefore, 50% of the span length of a beam may be considered the optimum length of wire mesh.

**Conclusion**

The FE approach is used to evaluate the bending behavior of reinforced concrete beams strengthened with wire mesh. The possibility of a concrete beam that has been partially or completely reinforced with steel wire is also being studied. The finite element model of the experimental beam is tested against the loading test results. The bending load performance of the beams is assessed in terms of load carrying

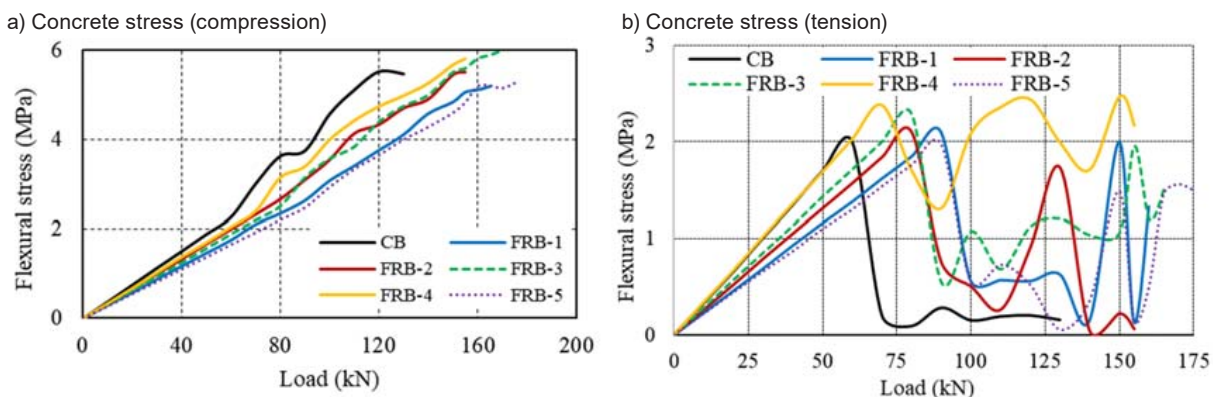


Fig. 16. Flexural stress at different retrofitted beams

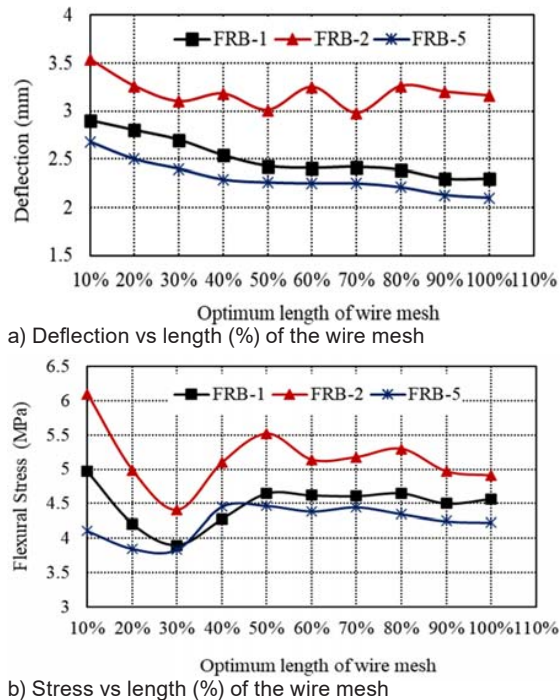


Fig. 17. Deflection and flexural stress for different lengths of the wire mesh

capacity, beam deflection, working stress, crack and crack depths, and wire mesh optimal length. The main findings of this research are briefly summarized below:

- A beam in which rebars are partially or completely replaced by steel wire or a steel-reinforced concrete beam strengthened with wire mesh has greater bending capacity than a conventional steel-reinforced concrete beam. The wire mesh increases the flexural capacity by 15%~43% at the first crack and 20%~35% at the ultimate load, which is significant when wire mesh is used along three sides of a beam.

- The deflection and concrete stress at the failure load level are large when regular reinforcement is replaced with an equal quantity of wire mesh by mass. The beam retrofitted with wire mesh has higher ductility and lower flexural stress.

- Wire mesh improves the flexural crack distribution and reduces the depth of flexural cracks.

The length of wire mesh equal to 50% of the span length is sufficient to reinforce a partially damaged beam, beyond which the concrete stress and beam deflection remain unaffected.

## References

- Adhikary, B. B. and Mutsuyoshi, H. (2006). Shear strengthening of reinforced concrete beams using various techniques. *Construction and Building Materials*, 20, pp. 366–373. DOI: <https://doi.org/10.1016/j.conbuildmat.2005.01.024>
- Anthony J. Wolanski, B.S. (2004). Flexural Behavior of Reinforced and Prestressed Concrete Beams Using Finite Element Analysis, *Master's Thesis*, Marquette, May, 2004.
- ANSYS Inc., Release 15.0 Documentation, Theory References, 2013.
- Ashraf, M., Khan, A. N., Naseer, A., Ali, Q., and Alam, B. (2012). Seismic behavior of unreinforced and confined brick masonry walls before and after ferrocement overlay retrofitting. *International Journal of Architectural Heritage*, 6(6), pp. 665–688. DOI: <https://doi.org/10.1080/15583058.2011.599916>.
- Abdullah and Takiguchi, K. (2003). An investigation into the behavior and strength of reinforced concrete columns strengthened with ferrocement jackets, *Cement and Concrete Composites*, 25(2), pp. 233–242. DOI: [https://doi.org/10.1016/S0958-9465\(02\)00005-7](https://doi.org/10.1016/S0958-9465(02)00005-7).
- Chanda, M., Zisan, M.B., Dhar, A. (2022). Flexural Behaviour of Reinforced Concrete Beams Retrofitted with Ferrocement. In: Arthur, S., Saitoh, M., Pal, S.K. (eds) *Advances in Civil Engineering. Lecture Notes in Civil Engineering*, vol 184. Springer, Singapore. DOI: 10.1007/978-981-16-5547-0\_24.
- El-Wafa, M. A., and Fukuzawa, K. (2008). Various sizes of wire mesh reinforcement effect on tensile behavior of ferrocement composite plates. *Proceedings of the 10<sup>th</sup> International Summer Symposium Organized*, JSCE, Tokyo, Japan.
- El-Wafa, M. A., and Fukuzawa, K. (2010). Characteristics of ferrocement thin composite elements using various reinforcement meshes in flexure. *Journal of Reinforced Plastic Composite*, 29(23), pp. 3530-3539. DOI: <https://doi.org/10.1177/0731684410377814>
- El-Sayed, T. A., and Erfan, A. M. (2018). Improving shear strength of beams using ferrocement composite. *Construction and Building Materials*, 172, pp. 608–617. DOI: <https://doi.org/10.1016/j.conbuildmat.2018.03.273>
- Faherty, K. F. (1972). An Analysis of a Reinforced and a Prestressed Concrete Beam by Finite Element Method. *Doctorate's Thesis*, University of Iowa, Iowa City.

- Fahmy, E. H., Shaheen, Y. M., and Zeid, A. (2004). Development of ferrocement panels for floor and wall construction, *5<sup>th</sup> Structural Specialty Conference of the Canadian Society for Civil Engineering*, Canada.
- Fahmy, E. H., Shaheen Y. B., Abou, Z.M.D., and Gaafar, A. M. (2012). Ferrocement sandwich and hollow core panels for floor construction. *Canadian Journal of Civil Engineering*, 27 (1), pp.1297–1310. DOI: <https://doi.org/10.1139/cjce-2011-0016>
- Fahmy, E. H., Shaheen, Y. B. I., and Abdelnaby, A. M. (2014). Applying the Ferrocement Concept in Construction of Concrete Beams Incorporating Reinforced Mortar Permanent Forms. *International Journal of Concrete Struct and Materials*, 8, pp. 83–97. DOI: <https://doi.org/10.1007/s40069-013-0062-z>
- Gaidhankar, D. G., Kulkarni, M. S., and Jaiswal, A. R. (2017). Ferrocement Composite Beams Under Flexure. *International Research Journal of Engineering and Technology*, 10, pp. 117–124.
- G.J. Al-Sulaimani, I.A. Basunbul, E.A. Mousselhy (1991). Shear behavior of ferrocement box beams. *Cement and Concrete Composites*, 13(1), pp. 29–36. DOI: [https://doi.org/10.1016/0958-9465\(91\)90044-l](https://doi.org/10.1016/0958-9465(91)90044-l)
- Hago, A. W., Al-Jabri, K. S., and Alnuaimi, A. S. (2005). Ultimate and service behavior of ferrocement roof slab panels. *Construction and Building Materials*, 19(1), pp. 31–37. DOI: <https://doi.org/10.1016/j.conbuildmat.2004.04.034>
- Hasan, M. A., Akiyama, M., Kashiwagi, K., Kojima, K., and Peng, L. (2020). Flexural behaviour of reinforced concrete beams repaired using hybrid scheme with stainless steel rebars and CFRP sheets. *Construction and Building Materials*, 208, pp. 228–241. DOI: <https://doi.org/10.1016/j.conbuildmat.2020.120296>
- Hasan, M. A., Akiyama, M., Kojima, K., and Izumi, N. (2022). Shear behavior of reinforced concrete beams repaired using hybrid scheme with stainless steel rebars and CFRP sheets. *Construction and Building Materials*, 363, 12817. DOI: <https://doi.org/10.1016/j.conbuildmat.2022.129817>
- Husein, N. R., Agarwal, V. C. and Rawat, A. (2013). An experimental study on using lightweight web sandwich panel as a floor and a wall, *International Journal of Innovative Technology and Exploring Engineering*, 3, pp. 2278–3075.
- Jamil, A. K., Zisan, M. B., Alam, M. R., and Alim, H. (2013). Restrengthening of RCC Beam by Beam Jacketing, *Malaysian Journal of Civil Engineering* 25(2), pp. 119-127. DOI: <https://doi.org/10.11113/mjce.v25.15847>.
- Kadir, M. A., Samad, A. A., Muda, Z. C. and Ali A. (1997). Flexural behavior of composite beam with ferrocement permanent formwork. *Journal of Ferrocement*, 27, pp. 209–214.
- Kaish, A. B. M. A., Alam, M. R., Zain, M. F. M., and Wahed, M. A. (2012). Improved ferrocement jacketing for restrengthening of square RC short column. *Construction and Building Materials*, 36, pp. 228–237. DOI: <https://doi.org/10.1016/j.conbuildmat.2012.04.083>.
- Kaish, A. B. M. A., Alam, M. R., Jamil, M. and Wahed, M. A. (2013). Ferrocement Jacketing for Restrengthening of Square Reinforced Concrete Column under Concentric Compressive Load, *Journal of Procedia Engineering*, 54, pp. 720 – 728. DOI: <https://doi.org/10.1016/j.proeng.2013.03.066>
- Kaish, A. B. M. A., Jamil, M., Raman S. N., Zain M. F. M. and Alam, M. R. (2016). An approach to improve conventional square ferrocement jacket for strengthening application of short square RC column. *Journal of Material and Structure*, 49, pp. 1025–1037. DOI: <https://doi.org/10.1617/s11527-015-0556-z>
- Kibria, B. M. G., Ahmed, F., and Ahsan, R. (2020). Experimental investigation on behavior of reinforced concrete interior beam column joints retrofitted with fiber reinforced polymers. *Asian Journal of Civil Engineering*, 21, pp. 157–171. DOI: <https://doi.org/10.1007/s42107-019-00204-3>
- Leeanansaksiri, A., Panyakapo, P., and Ruangrassamee A. (2018). Seismic capacity of masonry infilled RC frame strengthening with expanded metal ferrocement. *Engineering Structures*, 159, pp. 110–127. DOI: <https://doi.org/10.1016/j.engstruct.2017.12.034>.
- Li, B., and Lam, E. S. S. (2018). Influence of interfacial characteristics on the shear bond behaviour between concrete and ferrocement. *Construction and Building Materials*, 176, pp. 462–469. DOI: <https://doi.org/10.1016/j.conbuildmat.2018.05.084>
- Li, B., Lam, E. S. S., Wu, B., and Wang, Y. Y. (2013). Experimental investigation on reinforced concrete interior beam–column joints rehabilitated by ferrocement jackets. *Engineering Structures*, 56, pp. 897–909. DOI: <https://doi.org/10.1016/j.engstruct.2013.05.038>
- Mataalkah, F., Bharadwaj, H., and Soroushian, P. (2017). Development of sandwich composites for building construction with locally available materials. *Construction and Building Materials*, 147, pp. 380–387. DOI: <https://doi.org/10.1016/j.conbuildmat.2017.04.113>
- Muhit, I. B., Jitu, N. E. T., and Alam, A. R. (2021). Structural shear retrofitting of reinforced concrete beam: multilayer ferrocement technique. *Asian Journal of Civil Engineering*, 22, pp. 191–203. DOI: <https://doi.org/10.1007/s42107-020-00306-3>
- Niloy, S. H., and Islam, M. M. (2017). Flexural Behavior of Reinforced Concrete Beams Retrofitted with Ferrocement. *Bachelor's Thesis*, Chittagong University of Engineering & Technology, Chittagong, Bangladesh. Oehlers, D. J., Nguyen, N. T., and

- Bradford, M. A. (2000). Retrofitting by adhesive bonding steel plates to the sides of R.C. beams. Part 1: Debonding of plates due to flexure. *Structural Engineering and Mechanics*, 9(5), pp. 491–504. DOI: <https://doi.org/10.12989/SEM.2000.9.5.491>
- Obaidat, Y. T., Heyden, S., and Dahlblom, O. (2011). Retrofitting of reinforced concrete beams using composite laminates. *Construction and Building Materials*, 25(2), pp. 591–597. DOI: <https://doi.org/10.1016/j.conbuildmat.2010.06.082>
- Pham, H., and Al-Mahaidi, R. (2004). Experimental investigation into flexural retrofitting of reinforced concrete bridge beams using FRP composites. *Composite Structures*, 66(1–4), pp. 617–625. DOI: <https://doi.org/10.1016/j.compstruct.2004.05.010>
- Shaaban, I. G. (2002), Expanded Wire Fabric Permanent Formwork for Improving Flexural Behaviour of Reinforced Concrete Beams, *Proceedings of the International Congress: Challenges of Concrete Construction*, Dundee, Scotland, UK.
- Shaaban, I. G., Shaheen, Y. B., and Elsayed E. L. (2018). Flexural characteristics of lightweight ferrocement beams with various types of core materials and mesh reinforcement. *Construction and Building Materials*, 171, pp. 802–816. DOI: <https://doi.org/10.1016/j.conbuildmat.2018.03.167>
- Shaaban, I. G., Shaheen, Y. B. I., and Elsayed, E. L. (2013). Flexural behaviour and theoretical prediction of lightweight ferrocement composite beams. *Case Studies in Construction Materials*, 9, pp. e00204. DOI: <https://doi.org/10.1016/j.cscm.2018.e00204>
- Shaaban, I. G. and Seoud, O. A. (2018). Experimental behavior of full-scale exterior beam-column space joints retrofitted by ferrocement layers under cyclic loading, *Case Studies in Construction Materials*, 8, pp. 61–78. DOI: <https://doi.org/10.1016/j.cscm.2017.11.002>
- Shaheen, Y. B. I., and Eltehawy, E. A. (2017). Structural behaviour of ferrocement channels slabs for low-cost housing. *Challenge Journal of Concrete Research Letter*, 8 (2), pp. 48–64. DOI: <https://doi.org/10.20528/CJCRL.2017.02.002>
- Si, B.J., Sun, Z.G., Ai, Q.H., Wang, D.S., and Wang, Q.X, (2008). Experiments And Simulation Of Flexural-Shear Dominated Rc Bridge Piers Under Reversed Cyclic Loading, *The 14<sup>th</sup> World Conference on Earthquake Engineering*, Beijing, China.
- Sowmya, E., and Venkatasubramani, R. (2017). Numerical Study of Wire Mesh Orientation on Retrofitted RC Beams Using Ferrocement Jacketing. *International Research Journal of Engineering & Technology*, 4(11), pp.1471-1475.
- Tanaka T., Yagi K., and Kojima N. (1994). Retrofit method with carbon fiber for reinforced concrete structures, *Advanced Composite Materials*, 4(2), pp.183-195. DOI: 10.1163/156855194X00303.
- Tjitradi, D, Eliatun, E, and Taufik, S. (2017). 3D ANSYS Numerical Modeling of Reinforced Concrete Beam Behavior under Different Collapsed Mechanisms. *International Journal of Mechanics and Applications*, 7(1), pp.14-23. DOI: 10.5923/j.mechanics.20170701.02
- Van Cao, V., and Quoc Nguyen, T. (2019). Effects of CFRP/GFRP flexural retrofitting on reducing seismic damage of reinforced concrete frames: a comparative study. *Asian Journal of Civil Engineering*, 20, pp. 1071–1087. DOI: <https://doi.org/10.1007/s42107-019-00173-7>
- Yousef S. Al Rjoub, Ahmed M. Ashteyat, Yasmeen T. Obaidat & Saleh Bani-Youniss (2019). Shear strengthening of RC beams using near-surface mounted carbon fibre-reinforced polymers. *Australian Journal of Structural Engineering*, 20(1), pp. 54–62. DOI: <https://doi.org/10.1080/13287982.2019.156561>
- Zisan M. B., Haque, M. N., Chowdhury, M. S. U. (2011). A Finite Element Analysis for Optimization of Flexural Cracked Beam Strengthened using CFRP composites, *Proceedings of the International Conference on Mechanical Engineering and Renewable Energy 2011 (ICMERE2011) 22-24 December 2011, Chittagong, Bangladesh.*